

# A Mathematical model for analysing the transmission and control of COVID-19 infection with efficient interventions

Olawale J. Adeleke<sup>1,\*</sup>, Adebayo O. Adeniran<sup>1</sup>, Michael O. Olusanya<sup>2</sup>, Dimpho Mothibi<sup>3</sup>

<sup>1</sup>*Department of Mathematics and Statistics, Redeemer's University, Ede, Nigeria*

<sup>2</sup>*Department of Computer Science and Information Technology, Sol Plaatje University, Kimberly, Republic of South Africa*

<sup>3</sup>*Department of Mathematical Sciences, Sol Plaatje University, Kimberly, Republic of South Africa*

**Abstract** The COVID-19 pandemic, caused by SARS-CoV-2, continues to pose a significant global threat. Mathematical modelling offers a valuable tool for understanding transmission dynamics and designing control strategies. The recent emergence of new variants of the disease and the incidents of infections in people who had previously recovered from the disease have necessitated the need to study the control of the transmission of the disease in the face of re-infection. Thus, this study presents a novel compartmental model for the COVID-19 epidemic that incorporates the possibility of re-infection. The model captures the transition of individuals through susceptible, quarantined, exposed, infected, treated, and recovered compartments. Various mathematical analyses of the model were presented to provide the reading audience with vital information on the disease dynamics. Afterwards, we employed optimal control theory to identify interventions that minimise the infected population while considering the associated costs. By applying Pontryagin's Maximum Principle, we determine the optimal control strategies for these interventions. This framework allows us to evaluate the effectiveness of various control measures, such as minimal contact, early therapeutic treatment of infected individuals, quarantine, and vaccination, in mitigating the epidemic while accounting for the possibility of re-infection. Our findings can inform public health decision-making as they provide insights into the most effective strategies for controlling the transmission of COVID-19 in the presence of re-infection.

**Keywords** COVID-19, Re-infection, Mathematical model, Hamiltonian, Optimal control theory, Pontryagin's maximum principle.

**AMS 2010 subject classifications** 34H05, 92B05

**DOI:** 10.19139/soic-2310-5070-2117

## 1. Introduction

The emergence of the novel coronavirus disease caused by SARS-CoV-2 had a devastating impact globally [41]. The first detected cases of SARS-CoV-2 emerged in Wuhan, China, in December 2019, which suggested the name COVID-19 for the disease. Early cases were linked to a seafood market, suggesting a potential animal origin [41]. By January 2020, Chinese authorities had identified the novel coronavirus, and the World Health Organisation (WHO) had declared a public health emergency of international magnitude in late January [38]. COVID-19 spread rapidly, prompting lockdowns and border restrictions worldwide. Despite ongoing vaccination efforts, the virus continues to evolve, with considerations of re-infection influencing control strategies [1].

Understanding the transmission dynamics and developing effective control strategies remain crucial for mitigating the ongoing pandemic. Mathematical modelling offers a powerful tool to analyse these dynamics and

---

\*Correspondence to: Olawale J. Adeleke (Email: [vjadeleke@gmail.com](mailto:vjadeleke@gmail.com)). Department of Mathematics and Statistics, Redeemer's University, Ede, Nigeria

predict disease outbreaks. This article explores the application of mathematical modelling and optimal control theory to the COVID-19 epidemic, specifically considering the possibility of re-infection [23, 19].

A cornerstone of epidemic modelling is the SEIR (Susceptible-Exposed-Infectious-Recovered) framework, which categorises the population into compartments based on their infection status. Numerous studies have adapted this framework to capture the complexities of COVID-19. Studies like [12] incorporate an exposed carrier compartment to account for pre-symptomatic transmission, while [19] differentiates between symptomatic and asymptomatic infectious individuals for a more detailed analysis.

The ongoing COVID-19 pandemic has presented unprecedented challenges globally, necessitating robust mathematical models to understand and control its transmission dynamics (see [11]). Recent studies highlight the critical importance of incorporating reinfection possibilities into these models, as emerging evidence suggests that individuals previously infected with SARS-CoV-2 are not immune to reinfection [22, 35]. This aspect is crucial for designing effective public health interventions and vaccination strategies, as it impacts herd immunity thresholds and long-term epidemic trajectories [32]. Furthermore, understanding the implications of reinfection can help refine control measures, such as quarantine policies, social distancing protocols, and booster vaccination campaigns, to mitigate the spread of the virus more effectively [36]. Thus, developing comprehensive models that account for reinfection scenarios is imperative for informed decision-making and effective pandemic management [24]. In particular, this study considers a special case where individuals in the quarantined compartment can either be re-incorporated into the susceptible class or become infected and therefore transferred to the treatment compartment.

There exist many optimization techniques for analysing and solving real-world problems (see [9, 15, 16, 28, 2, 3]) including epidemiological problems, many of which have been used to achieve great level of success in providing solutions to problems that have defied quality solutions for quite a long time. However, within the sphere of epidemiological research, mathematical models constitute potent tools that can be leveraged for optimal control, where interventions are optimized to achieve a desired outcome (see [5, 6, 7]). Studies like [17] employ optimal control theory to identify interventions that minimize infection spread while considering costs. This framework allows for evaluating the effectiveness of various control measures, such as social distancing, vaccination, and isolation protocols.

As the pandemic evolves, so too do the models. Recent research focuses on incorporating factors like emergence of new variants, waning immunity, and the impact of vaccination campaigns. Additionally, the social and economic consequences of control strategies are increasingly being factored into the models, making them more comprehensive tools for decision-making [23, 19, 12, 20, 34].

This article contributes to this ongoing research by proposing a mathematical model for COVID-19 that considers re-infection and utilizes optimal control theory to identify the most effective interventions for mitigating the epidemic.

## 2. The Model

Considering a homogeneous population at time  $(t)$ , the total population  $N(t)$  is divided into seven(7) epidemiological stages depending on individual health status; Susceptible Individual (S), Exposed Individual (E), Quarantined uninfected contacts (F), Asymptomatic infected individuals (A), Symptomatic infected individuals (I), Treated individuals (T), Recovered individuals (R). The total population ( $N$ ) at any time ( $t$ ) can be expressed as

$$N(t) = S(t) + E(t) + A(t) + I(t) + Q(t) + T(t) + R(t) \quad (1)$$

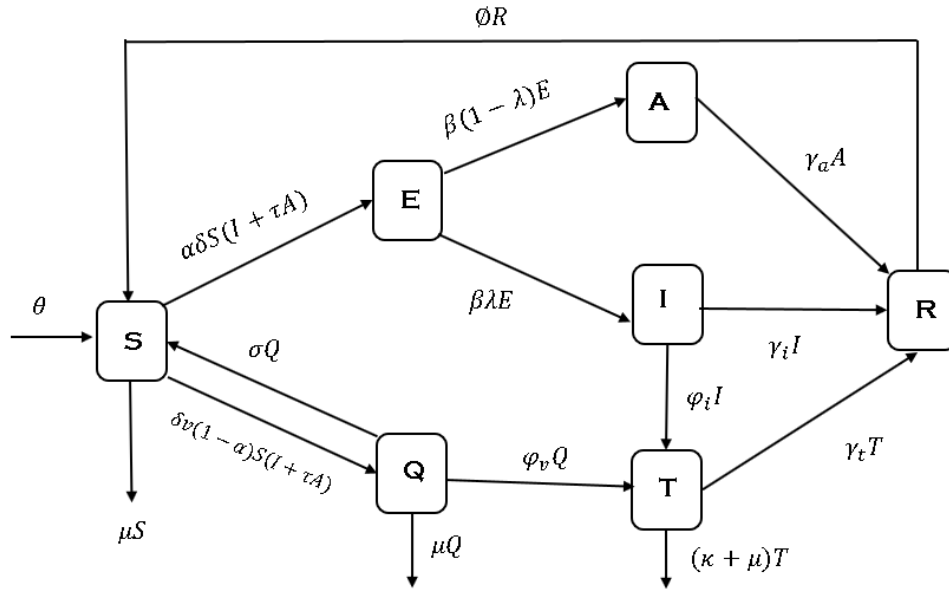


Figure 1. Model diagram showing the transmission of COVID-19

Table 1. Description of model parameters .

Parameter	Descriptions	value	Reference
$S$	Susceptible individual		
$E$	Exposed individuals		
$Q$	Quarantined uninfected contacts		
$A$	Asymptomatic infected individuals		
$I$	Symptomatic infected individuals		
$T$	Treated individuals		
$R$	Recovered individuals		
$\delta$	contact rate	0.0510	[26]
$\alpha$	probability of transmission per contact	0.01	[26]
$\nu$	quarantined rate of exposed individuals	0.012	[26]
$\beta$	transition rate of exposed to infected	0.25	[33]
$\sigma$	transition rate from quarantined uninfected to susceptible	0.02	[8]
$\lambda$	probability of having symptom among infected individuals	0.04	[39]
$\kappa$	disease-induced death rate	0.06	[33]
$\mu$	natural death rate	0.1512	[8]
$\tau$	probability of exposure to asymptomatic infected individuals	0.02	Assumed
$\varphi_i$	transfer rate from symptomatic infected to treated individuals	0.03	[39]
$\varphi_v$	transfer rate of quarantined infected to treated individuals	0.4	[40]
$\phi$	transfer rate of recovered individuals to susceptible individuals	0.4	[40]
$\theta$	recruitment rate of new susceptible individuals	1000	Assumed
$\gamma_i$	recovery rate of infected individuals	0.03	[33]
$\gamma_a$	recovery rate of asymptomatic infected individuals	0.1	Assumed
$\gamma_t$	recovery rate of treated infected individuals	0.8	[8]

From the description of model parameters in Table 1 and the compartmental diagram in Figure 1, we have the following system of differential equation.

$$\begin{aligned}
 \frac{dS}{dt} &= \theta - \alpha\delta S(I + \tau A) - \delta\nu(1 - \alpha)S(I + \tau A) - \mu S + \sigma Q + \phi R \\
 \frac{dE}{dt} &= \alpha\delta S(I + \tau A) - \beta E \\
 \frac{dI}{dt} &= \beta\lambda E - (\gamma_1 - \varphi_i)I \\
 \frac{dA}{dt} &= \beta(1 - \lambda)E - \gamma_a A \\
 \frac{dQ}{dt} &= \delta\nu(1 - \alpha)S(I + \tau A) - (\sigma + \varphi_\nu + \mu)Q \\
 \frac{dT}{dt} &= \varphi_\nu Q + \varphi_i I - (\delta_t + \kappa + \mu)T \\
 \frac{dR}{dt} &= \delta_a A + \delta_i I + \delta_t T - \phi R \\
 S(0) &= S_o, E(0) = E_o, I(0) = I_o, A(0) = A_o, Q(0) = Q_o, T(0) = T_o, R(0) = R_o.
 \end{aligned} \tag{2}$$

### 3. Model analysis

Studying simplified versions of how diseases spread helps us grasp and anticipate real-life outbreaks. These models, even if they are not perfect, give us important clues about how diseases move through a population and can be used to design public health measures.

#### 3.1. Dynamics of the model

With reference to equation (1), we have

$$\begin{aligned}
 \frac{dN}{dt} &= \frac{dS}{dt} + \frac{dE}{dt} + \frac{dI}{dt} + \frac{dA}{dt} + \frac{dQ}{dt} + \frac{dT}{dt} + \frac{dR}{dt} \\
 &= \theta - \mu(S + Q + T) - \kappa T.
 \end{aligned}$$

Assume  $N \cong S + Q + T$ , we have

$$\frac{dN}{dt} = \theta - \mu N - \kappa T. \tag{3}$$

Equation (3) describes the dynamics of the model.

#### 3.2. Boundedness of the model

In this section, the feasibility of the model which describes the region in which the solution of model (2) is investigated.

##### Lemma 3.1

Let  $(S, E, A, I, Q, T, R)$  be the solution of the system (2) with initial condition in a biologically feasible region  $\Omega$  with

$$\Omega = \{S, E, A, I, Q, T, R \in \mathbb{R}^7\},$$

then  $\Omega$  is non-negative invariant.

*Proof*

From equation (3), a change in  $N$  leads to change in all the variables in the population, in the absence of the disease, there is no need for treatment ( $\kappa = 0$ ), we have

$$\frac{dN}{dt} \leq \theta - \mu N. \quad (4)$$

Solving the differential inequality (4), yields

$$N(t) \leq N(t)e^{-\mu t} + \frac{\theta}{\mu} (1 - e^{-\mu t}). \quad (5)$$

As  $t \rightarrow \infty$

$$N(t) \leq \frac{\theta}{\mu}, \quad (6)$$

hence, the feasible solution region is given by

$$\Omega = \left\{ (S, E, A, I, Q, T, R) \in \mathbb{R}_+^7; N(t) \leq \frac{\theta}{\mu} \right\}.$$

Thus, the feasible region defined by  $\Omega$  is positively invariant.  $\square$

### 3.3. Positivity of solutions

*Lemma 3.2*

Let  $S(0), E(0), A(0), I(0), Q(0), T(0), R(0)$ , be the initial conditions of the system (2), then the solution of  $S, E, A, I, Q, T, R$  are nonnegative  $\forall t > 0$ .

*Proof*

Considering the first equation of system (2)

$$\begin{aligned} \frac{dS}{dt} &= \theta - \alpha\delta S(I + \tau A) - \delta\nu(1 - \alpha)S(I + \tau A) - \mu S + \sigma Q + \phi R, \\ &= \theta - [\alpha\delta(I + \tau A) + \delta\nu(1 - \alpha)(I + \tau A)] S - \mu S + \sigma Q + \phi R. \end{aligned} \quad (7)$$

Let  $P = [\alpha\delta(I + \tau A) + \delta\nu(1 - \alpha)(I + \tau A)]$ , then,

$$\frac{dS}{dt} = \theta - PS - \mu S + \sigma Q + \phi R. \quad (8)$$

Thus,

$$\frac{dS}{dt} \geq -(P + \mu)S. \quad (9)$$

On integrating (9), we have

$$S(t) \geq e^{-(P+\mu)t} e^C,$$

where  $C$  is a constant of integration. Let  $B = e^C$ , we have

$$S(t) \geq B e^{-(P+\mu)t}. \quad (10)$$

At  $t = 0$ , equation (10) is reduced to

$$S(0) \geq B. \quad (11)$$

Substituting equation (11) into (10), we have

$$S(t) \geq S(0)e^{-(P+\mu)t}. \quad (12)$$

Hence,  $S(t) \geq 0$ , since  $(P + \mu) > 0$ . Thus,

$$S(t) \geq 0 \quad \forall t > 0.$$

In a similar approach, we prove the remaining equations of equation (2).

Thus,

$$S(t) \geq 0, \quad E(t) \geq 0, \quad I(t) \geq 0, \quad A(t) \geq 0, \quad Q(t) \geq 0, \quad T(t) \geq 0, \quad R(t) \geq 0.$$

That is, all the solutions are nonnegative  $\forall t > 0$ . □

### 3.4. Equilibrium of Solution

Let  $E = (S, E, I, A, Q, T, R) \in \Omega$  be the equilibrium point of the system (2), that is,

$$\frac{dS}{dt} = \frac{dE}{dt} = \frac{dI}{dt} = \frac{dA}{dt} = \frac{dQ}{dt} = \frac{dT}{dt} = \frac{dR}{dt} = 0$$

At equilibrium, equation (2) becomes

$$\begin{aligned} \theta - \alpha\delta S(I + \tau A) - \delta\nu(1 - \alpha)S(I + \tau A) - \mu S + \sigma Q + \phi R &= 0 \\ \alpha\delta S(I + \tau A) - \beta E &= 0 \\ \beta\lambda E - (\gamma_1 - \varphi_i)I &= 0 \\ \beta(1 - \lambda)E - \gamma_a A &= 0 \\ \delta\nu(1 - \alpha)S(I + \tau A) - (\sigma + \varphi_\nu + \mu)Q &= 0 \\ \varphi_\nu Q + \varphi_i I - (\delta_t + \kappa + \mu)T &= 0 \\ \delta_a A + \delta_i I + \delta_t T - \phi R &= 0. \end{aligned} \tag{13}$$

Solving (13), we shall obtain two equilibria: the disease free equilibrium  $\mathbb{E}^+ = (S^+, E^+, I^+, A^+, Q^+, T^+, R^+)$  and endemic equilibrium  $\mathbb{E}^* = (S^*, E^*, I^*, A^*, Q^*, T^*, R^*)$

#### *Disease free equilibrium of the model:*

In a model that tracks how a disease spreads, a disease-free equilibrium (DFE) is a situation where nobody has the disease, and it stays that way. This basically means the disease vanishes from the population entirely. Scientists use these models to understand how diseases move through people over time [13].

Solving equation (13) and letting  $E^+ = I^+ = A^+ = Q^+ = T^+ = R^+ = 0$ , that is, in the absence of the disease,

$$S^+ = \frac{\theta}{\mu},$$

so that

$$\mathbb{E}^+ = (S^+, E^+, I^+, A^+, Q^+, T^+, R^+) = \left( \frac{\theta}{\mu}, 0, 0, 0, 0, 0, 0 \right) \tag{14}$$

#### *Endemic Equilibrium:*

Endemic equilibrium state is the state where the disease persist in the population. At endemic equilibrium, we solve equation (13) simultaneously for  $S^*, E^*, I^*, A^*, Q^*, T^*, R^*$ .

$$\begin{aligned} S^* &= \frac{\gamma_a(\gamma_i + \varphi_i)}{\alpha\delta[\lambda\gamma_a + \tau(1 - \lambda)(\gamma_i + \varphi_i)]} \\ E^* &= \frac{(\gamma_i + \varphi_i)\theta_1}{\beta\lambda\theta_2} \end{aligned}$$

$$\begin{aligned}
I^* &= \frac{\theta_1}{\theta_2} \\
A^* &= \frac{\theta_1(1-\lambda)(\gamma_i + \varphi_j)\theta_1}{\theta_2\gamma_a\theta_2} \\
Q^* &= \frac{\nu(1-\alpha)(\gamma_i + \varphi_i)\theta_1}{\alpha\lambda(\sigma + \varphi_v\mu)\theta_2} \\
T^* &= \frac{[\varphi_v\nu(1-\alpha)(\gamma_i + \varphi_i) + \alpha\lambda\varphi_i(\sigma + \varphi_v + \mu)]\theta_1}{\alpha\lambda(\sigma + \varphi_v + \mu)(\gamma_t + \kappa + \mu)\theta_2} \\
R^* &= \frac{(1-\lambda)(\gamma_i + \varphi_i)\theta_1}{\lambda\phi\theta_2} + \frac{\gamma_i\theta_1}{\varphi\theta_2} + \frac{\gamma_t\theta_1[\varphi_v\nu(1-\alpha)(\gamma_i + \varphi_i) + \alpha\lambda\varphi_i(\rho + \varphi_v + \mu)]\theta_1}{\alpha\lambda\phi(\sigma + \varphi_v + \mu)(\gamma_t + \kappa + \mu)\theta_2}
\end{aligned}$$

where

$$\begin{aligned}
\theta_1 &= \lambda H_4 H_6 [\alpha\delta\theta(\lambda\varphi_a + H_2 H_3) - \mu\varphi_a H_2] \\
\theta_1 &= \delta [\lambda\gamma_t + H_2 H_3] [\alpha H_4 (H_2 H_6 - H_6 \gamma_i - H_5 H_6 - \lambda\varphi_i \gamma_t) + H_1 H_2 (H_6 - H_2 \rho - \gamma_t \varphi_v)] \\
H_1 &= \nu(1-\alpha), & H_2 &= \gamma_i + \varphi_i \\
H_3 &= \tau(1-\lambda), & H_4 &= \rho + \varphi_v + \mu \\
H_5 &= \varphi_i(1-\lambda), & H_6 &= \varphi_t + \kappa + \mu
\end{aligned}$$

#### 4. Basic Reproduction Number

In the study of infectious diseases, a number called the "basic reproduction number", tells us how easily a disease can spread.

The basic reproduction number, often abbreviated as  $R_o$ , is a key concept in epidemiology. it's a measure of how contagious a disease is, a higher  $R_o$  means that each infected pod, on average, infects more pods, leading to a faster spread of the disease. Conversely, a lower  $R_o$  indicates that the disease is less contagious and will spread more slowly [37]. For instance, if a disease has an  $R_o$  of 3, then one infected person can be expected to transmit the disease to 3 other people on average.

$R_o$  greater than 1 indicates that the infection will spread exponentially. Conversely, an  $R_o$  less than 1 means that the infection will die out. The concept is instrumental in understanding the spread of infectious diseases and implementing control measures. Public health interventions like vaccination aim to bring down the  $R_o$  below 1 to stop the spread of a disease.

According to [37], factors affecting the basic reproduction number are:

- **infectiousness of the disease:** this refers to how easily a disease can be transmitted from one person to another.
- **duration of the infectious period:** the longer an infected person remains contagious, the higher the chance of transmission.
- **rate of contact between susceptible individuals and infected individuals:** this depends on various factors like population density, social mixing patterns, and hygiene practices.

$R_o$  is the average number of secondary infections caused by a single infected individual in a population that is entirely susceptible to the disease [37]. Computation of  $R_o$  is carried out using the next generation matrix as laid out in [37].  $R_o$  is obtained using

$$R_o = \rho(FV^{-1}), \quad (15)$$

where  $\rho$  is the spectral radius of the matrix  $FV^{-1}$ . Differential equations which is associated with  $E$ ,  $I$ ,  $A$ , and  $Q$  compartments are the infective classes and will be used in the computation of  $R_o$ .

$$\begin{aligned}\frac{dE}{dt} &= \alpha\delta S(I + \tau A) - \beta E, & \frac{dI}{dt} &= \beta\lambda E - (\gamma_1 + \varphi_i)I, & \frac{dA}{dt} &= \beta(1 - \lambda)E - \gamma_a A, \\ \frac{dQ}{dt} &= \delta\nu(1 - \alpha)S(I + \tau A) - (\sigma + \varphi_\nu + \mu)Q, & \frac{dT}{dt} &= \varphi_\nu Q + \varphi_i I - (\delta_t + \kappa + \mu)T.\end{aligned}\quad (16)$$

From system (16), we derive

$$F_i = \begin{pmatrix} \alpha\delta S(I + \tau A) \\ 0 \\ 0 \\ \delta\nu(1 - \alpha)S(I + \tau A) \end{pmatrix}, V_i = \begin{pmatrix} \beta E \\ -\beta\lambda E + (\gamma_i + \varphi_i)I \\ -\beta(1 - \lambda)E + \gamma_a A \\ (\sigma + \varphi_\nu + \mu)Q \\ -\varphi_i I + (\gamma_t + \kappa + \mu)T \end{pmatrix}.$$

Computing the partial derivative of  $F_i$  and  $V_i$  with respect to  $E, I, A, Q, T$ , we obtain

$$F = \begin{pmatrix} 0 & \alpha\delta S & \alpha\delta\tau S & 0 & 0 \\ 0 & 0 & 0 & 0 & 0 \\ 0 & 0 & 0 & 0 & 0 \\ 0 & \delta\nu(1 - \alpha)S & \delta\nu(1 - \alpha)\tau S & 0 & 0 \\ 0 & 0 & 0 & 0 & 0 \end{pmatrix},$$

$$V = \begin{pmatrix} \beta & 0 & 0 & 0 & 0 \\ -\beta\lambda & (\gamma_i + \varphi_i) & 0 & 0 & 0 \\ \beta(1 - \lambda) & 0 & \gamma_a & 0 & 0 \\ 0 & 0 & 0 & (\sigma + \varphi_\nu + \mu) & 0 \\ 0 & -\varphi_i & 0 & \varphi_\nu & (\gamma_t + \kappa + \mu) \end{pmatrix}.$$

With respect to equation (15),  $R_o$ , which is the dominant eigenvalue of equation is obtained as

$$R_o = \frac{\alpha\delta\theta [\lambda\gamma_a + \tau(1 - \lambda)(\gamma_i + \varphi_i)]}{(\gamma_i + \varphi_i)\gamma_a\mu}, \quad (17)$$

equation (17) is the basic reproduction number for model (2)

- (i) whenever  $R_o > 1$ , it indicates that each infected person, on average, will infect more than one other person, leading to an outbreak.
- (ii) Whenever  $R_o < 1$ , it means that the disease will likely die out on its own, as each infected person, on average, infects fewer than one other person.
- (iii) Whenever  $R_o = 1$ , it indicates new cases remains constant, neither increasing nor decreasing, the outbreak is not actively growing, but it's not dying out either.

## 5. Stability Analysis

### 5.1. Local stability analysis of the disease free equilibrium

#### Lemma 5.1

Whenever  $R_o < 1$ , the disease free equilibrium  $\mathbb{E}^+$  is locally asymptotically stable, otherwise it is unstable.



*Proof*

The Jacobian matrix  $J$  of model (2) will be computed by differentiating each equation in system with respect to state variables  $S, E, I, A, Q, T, R$ . The model system (2) linearized around the DFE solution (14) yields the Jacobian matrix below:

$$J^+ = \begin{pmatrix} -\mu & 0 & -\psi_1 S^+ & -\psi_2 S^+ & 0 & 0 & \phi \\ 0 & -\beta & \psi_4 & \psi_5 S^+ & 0 & 0 & 0 \\ 0 & \psi_3 & -\psi_6 & 0 & 0 & 0 & 0 \\ 0 & \psi_7 & 0 & -\gamma_a & 0 & 0 & 0 \\ 0 & 0 & \psi_8 S^+ & \psi_9 & -\psi_{10} & 0 & 0 \\ 0 & 0 & \varphi_i & 0 & \varphi_v & -\psi_{11} & 0 \\ 0 & 0 & \gamma_i & \gamma_a & 0 & \gamma_t & -\phi \end{pmatrix}, \quad (18)$$

where  $\psi_1 = [\alpha + \nu(1 - \alpha)] \delta$ ,  $\psi_2 = [\alpha + \nu(1 - \alpha)] \delta \kappa$ ,  $\psi_3 = \beta \lambda$ ,  $\psi_4 = \alpha \delta$ ,  $\psi_5 = \alpha \delta \tau$ ,

$\psi_6 = \gamma_i + \varphi_i$ ,  $\psi_7 = \beta(1 - \lambda)$ ,  $\psi_8 = \delta \kappa(1 - \alpha)$ ,  $\psi_9 = \delta \kappa(1 - \alpha) \tau$ ,  $\psi_{10} = \sigma + \varphi_v + \mu$ ,  $\psi_{11} = \gamma_t + \kappa + \mu$ .

Matrix  $J^+$  in equation (18) above is stable if its trace is negative,  $\text{tr}(J^+) < 0$  and its determinant is positive,  $\det(J^+) > 0$ . Here,  $\text{tr}(J^+)$  is computed as

$$\begin{aligned} \text{tr}(J^+) &= -(\mu + \beta + \psi_6 + \gamma_a + \psi_{10} + \psi_{11}) \\ &= -(3\mu + \beta + \gamma_i + \varphi_i + \delta_a + \rho + \varphi_v + \gamma_t + \kappa) \end{aligned}$$

Therefore,  $\text{tr}(J^+) < 0$ .

Likewise, the determinant of matrix ( $J^+$ ) in equation (18) is given as

$$\det(J^+) = \left[ \psi_6 \psi_5 \frac{\theta}{\mu} \beta + \psi_4 \beta \lambda \gamma_a - \psi_6 \beta \left( \gamma_a + \lambda \psi_5 \frac{\theta}{\beta} \right) \psi_{10} \psi_{11} \phi \mu \right].$$

Therefore,  $\det(J^+) \geq 0$ , if

$$\psi_6 \psi_5 \frac{\theta}{\mu} \beta + \psi_4 \beta \lambda \gamma_a \geq \psi_6 \beta \left( \gamma_a + \lambda \psi_5 \frac{\theta}{\beta} \right)$$

Thus  $J^+$  will be stable and asymptotically stable if the condition above is satisfied.  $\square$

## 5.2. Global stability analysis of the disease free equilibrium

In this subsection, the global stability of the disease free equilibrium ( $\mathbb{E}^+$ ) will be discussed with the aid of Lyapunov function (see [10] for more details).

*Lemma 5.2*

Disease free equilibrium of the system (2) is globally asymptotically stable if  $R_o \leq 1$ ,  $\theta = \mu N$  and unstable when  $R_o \geq 1$ .

*Proof*

The quadratic composite is used as the Lyapunov candidate as follows.

$$V = \frac{1}{2} [(S - S^+) + (E - E^+) + (I - I^+) + (A - A^+)(S - S^+) + (Q - Q^+) + (R - R^+)]^2 \quad (19)$$

Differentiating equation (19) with respect to time yields

$$\begin{aligned} \frac{dV}{dt} &[(S - S^+) + (E - E^+) + (I - I^+) + (A - A^+)(S - S^+) + (Q - Q^+) + (R - R^+)] \left( \frac{dS}{dt} + \frac{dE}{dt} + \right. \\ &\quad \left. \frac{dI}{dt} + \frac{dA}{dt} + \frac{dQ}{dt} + \frac{dT}{dt} + \frac{dR}{dt} \right) \end{aligned}$$

$$\frac{dV}{dt} [(S - S^+) + (E - E^+) + (I - I^+) + (A - A^+)(S - S^+) + (Q - Q^+) + (R - R^+)] \frac{dN}{dt}$$

At DFE,  $S^+ = \frac{\theta}{\mu}$ ,  $E^+ = I^+ = Q^+ = T^+ = R^+ = 0$  and  $\frac{dN}{dt} = \theta - \mu N - \kappa T$

$$\frac{dN}{dt} = \left[ S + E + I + A + Q + T + R - \frac{\theta}{\mu} \right] [\theta - \mu N - \kappa T]$$

$$\frac{dN}{dt} = \left[ N - \frac{\theta}{\mu} \right] [\theta - \mu N - \kappa T]$$

setting  $T = 0$

$$\frac{dN}{dt} \leq \left[ N - \frac{\theta}{\mu} \right] [\theta - \mu N]$$

$$\frac{dN}{dt} \leq -\frac{1}{\mu} [\theta - \mu N]^2$$

$$\frac{dN}{dt} \leq 0.$$

Hence,  $\frac{dN}{dt} \leq 0$ , if and only if  $\theta = \mu N$  and  $\mu > 0$ . □

## 6. Sensitivity analysis

Sensitivity indices allow us to measure the relative change in a variable when a parameter changes. The normalized forward sensitivity index of a variable to a parameter is the ratio of the relative change in the variable to the relative change in the parameter. When the variable is a differentiable function of the parameter, the sensitivity may be alternatively defined using partial derivatives

The normalized forward sensitivity index of a variable  $W$  that depends on a parameter  $M$  is defined as (see [4, 14, 37] for more details.)

$$Z_M^W = \frac{\partial W}{\partial M} \times \frac{M}{W}$$

The sensitivity analysis of  $R_o$  corresponding to the following parameters:  $\theta$ ,  $\alpha$ ,  $\delta$ ,  $\lambda$ ,  $\gamma_a$ ,  $\tau$ ,  $\gamma_i$ ,  $\varphi_i$  and  $\mu$  is obtained in the Table 2.

The indices with positive signs increases the value of  $R_o$  when they are increased and those with negative signs decreases the value of  $R_o$  when they are increased.

Understanding how a disease spreads is key to stopping it. This usually help to choose the best way to control the disease.

Table 2. Sensitivity Indices of  $R_o$

Parameter	Value	Sensitivity index
$\theta$	1000	+1.0000
$\alpha$	0.01	+1.0000
$\delta$	0.0510	+1.0000
$\lambda$	0.50	+0.6667
$\gamma_a$	0.02	-0.3333
$\tau$	0.02	+0.3333
$\gamma_i$	0.05	-0.1111
$\varphi_1$	0.40	-0.8889
$\mu$	0.1512	+1.0000

The value with negative index is an important parameter employed in the control of the disease because the value of  $R_o$  grows when the index with a positive indication is increased and decreases when the index with a negative indication is increased.

## 7. Analysis of optimal control

Instead of just predicting how an epidemic unfolds, optimal control theory empowers us to influence its course. It identifies the most effective interventions (control strategies) to achieve a specific goal [31]. This approach, like steering a ship, guides outbreaks towards desirable outcomes. Pontryagin's Maximum Principle (PMP) [29], a well-established method in biology and optimal control, provides the mathematical framework for this strategy.

The optimal control in this paper focuses on:

- (i)  $u_1$ : minimum contact;
- (ii)  $u_2$ : early therapeutic treatment of infected individuals;
- (iii)  $u_3$ : early quarantine
- (iv)  $u_4$ : vaccination.

Incorporating the above controls into model (2), we have

$$\begin{aligned}
 \frac{dS}{dt} &= \theta - (1 - u_1)\alpha\delta(I + \tau A)S [\delta\nu(1 - \alpha)(I + \tau A) + u_4] S - \mu S + \rho Q + \phi R \\
 \frac{dE}{dt} &= \alpha\delta S(I + \tau A) - \beta E \\
 \frac{dI}{dt} &= \beta\lambda E - (\gamma_1 - \varphi_i + u_2)I \\
 \frac{dA}{dt} &= (\beta(1 - \lambda) + u_3) E - \gamma_a A \\
 \frac{dQ}{dt} &= (\delta\nu(1 - \alpha)(I + \tau A) + u_4) S - (\sigma + \varphi_\nu + \mu + u_3)Q \\
 \frac{dT}{dt} &= (\varphi_\nu + u_3) Q + \varphi_i I - (\delta_t + \kappa + \mu + u_2)T \\
 \frac{dR}{dt} &= \gamma_a A + (\delta_i + u_2) I + \gamma_t T - \phi R
 \end{aligned} \tag{20}$$

Our goal is to find the most effective way to control COVID-19 spread and reduce infections. We want to achieve this by:

- (i) Minimizing contact: This means encouraging people to interact less frequently and at a safer distance.
- (ii) Early vaccination: Vaccinating as many people as possible as soon as they are eligible.
- (iii) Therapeutic treatment: Providing effective medications to those who become infected.
- (iv) Quick quarantine: Isolating infected individuals to prevent further transmission.

By focusing on these control measures, we aim to:

- Reduce the number of susceptible individuals becoming exposed to the virus.
- Lower the overall number of infected people.
- Minimize the need for lengthy quarantines.
- Increase the number of treated and recovered individuals.

The Objective functional for the minimization problem is expressed as

$$J = \min \int_0^T \left( A_1 S(t) + A_2 E(t) + A_3 I(t) + A_4 Q(t) + \frac{1}{2} \sum_{i=1}^4 B_i u_i^2(t) \right) dt, \quad (21)$$

subject to the constraint given in equation (20),  $T$  is a representation of the anticipated completion time for the controls implementation. where  $A_1, A_2, A_3$  and  $A_4$  are positive weight constants corresponding to  $S, E, I$  and  $Q$ . While  $B_1, B_2, B_3$  and  $B_4$  are the coefficient for each control measures. The terms  $B_1 u_1^2, B_2 u_2^2, B_3 u_3^2$ , and  $B_4 u_4^2$ , represent the cost associated with practice of minimizing contact, therapeutic treatment, early quarantine and vaccination respectively. Similar to previous research [18, 21, 25, 27], the cost control functions in this study adopt a quadratic form and the square of the control variables is taken to remove the severity of the control applied and the side effects of the therapeutic treatment.

In order to achieve our set objectives, we seek an optimal control triple,  $u^* = (u_i^*), i = 1, 2, 3, 4$  such that

$$J(u^*) = \min \{J(u_1, u_2, u_3, u_4 | u_i \in U)\}, \quad (22)$$

where  $U = \{u_i(t) : 0 \leq u_i(t) \leq 1, \text{Lebesgue measurable}, t \in [0, T]\}$ , is a non empty control set.

The lower bounds for  $u_i$  corresponds to no control measures applied, while the upper bound associated to be maximum effort exerted to minimize the transmission of COVID and other related cost.

### The Hamiltonian:

The Hamiltonian(H) for the control is defined as:

$$\begin{aligned} H(S, E, I, Q, A, I, R) = & A_1 S + A_2 E + A_3 I + A_4 Q + \frac{1}{2} (B_1 u_1^2 + B_2 u_2^2 + B_3 u_3^2 + B_4 u_4^2) + \\ & \lambda_1 \frac{dS}{dt} + \lambda_2 \frac{dE}{dt} + \lambda_3 \frac{dI}{dt} + \lambda_4 \frac{dA}{dt} + \lambda_5 \frac{dQ}{dt} + \lambda_6 \frac{dT}{dt} + \lambda_7 \frac{dR}{dt}. \end{aligned} \quad (23)$$

### Characterization of the optimal control solutions

Here, we characterize the optimal control  $u_1^*, u_2^*, u_3^*, u_4^*$ , which gives the optimal value for the control measures and the corresponding state variables  $(S^*, E^*, I^*, A^*, Q^*, T^*, R^*)$ . The necessary condition for the optimal control are obtained using PMP [30] to the Hamiltonian in equation (23). The principle transform the system of equation (20) and (21) into a problem minimizing pointwise Hamiltonian function and the adjoint variables  $\lambda$ 's with respect to the control functions  $u_1, u_2, u_3$  and  $u_4$ .

#### Lemma 7.1

Necessary Condition: Supposing that  $(S^*, E^*, I^*, A^*, Q^*, T^*, R^*)$  are optimal state solutions and  $(u_1, u_2, u_3, u_4)$  are associated optimal control variables for the optimal control problem (20), then there exist seven (7) adjoint variables  $\lambda_i$ , for  $i = 1, 2, \dots, 7$  which satisfy  $\frac{\partial \lambda_i}{\partial t} = -\frac{\partial H}{\partial x_i}$ , that is,

$$\begin{aligned} \frac{d\lambda_1}{dt} &= -\frac{\partial H}{\partial S} \\ \frac{d\lambda_2}{dt} &= -\frac{\partial H}{\partial E} \\ \frac{d\lambda_3}{dt} &= -\frac{\partial H}{\partial I} \\ \frac{d\lambda_4}{dt} &= -\frac{\partial H}{\partial A} \\ \frac{d\lambda_5}{dt} &= -\frac{\partial H}{\partial Q} \end{aligned} \quad (24)$$

$$\begin{aligned}\frac{d\lambda_6}{dt} &= -\frac{\partial H}{\partial T} \\ \frac{d\lambda_7}{dt} &= -\frac{\partial H}{\partial R}\end{aligned}$$

*Proof*

Using PMP, the adjoint conditions can be determined using the differential equation governing the adjoint variables along the transversality conditions. The adjoint equations are given by equation (24) with the transversality conditions

$$\lambda_1(T) = \lambda_2(T) = \lambda_3(T) = \lambda_4(T) = \lambda_5(T) = \lambda_6(T) = \lambda_7(T).$$

Recall from Equation (23)

$$\begin{aligned}H &= A_1 S + A_2 E + A_3 I + A_4 Q + \frac{1}{2} (B_1 u_1^2 + B_2 u_2^2 + B_3 u_3^2 + B_4 u_4^2) + \\ &\lambda_1 [\theta - (1 - u_1)\alpha\delta(I + \tau A)S [\delta\nu(1 - \alpha)(I + \tau A) + u_4] S - \mu S + \rho Q + \phi R] + \\ &\lambda_2 [\alpha\delta S(I + \tau A) - \beta E] + \lambda_3 [\beta\lambda E - (\gamma_1 - \varphi_i + u_2)I] + \\ &\lambda_4 [(\beta(1 - \lambda) + u_3) E - \gamma_a A] + \lambda_5 [(\delta\nu(1 - \alpha)(I + \tau A) + u_4) S - (\sigma + \varphi_\nu + \mu + u_3)Q] + \\ &\lambda_6 [(\varphi_\nu + u_3) Q + \varphi_i I - (\delta_t + \kappa + \mu + u_2)T] + \lambda_7 [\gamma_a A + (\delta_i + u_2) I + \gamma_t T - \phi R].\end{aligned}$$

Thus,

$$\begin{aligned}-\frac{\partial H}{\partial S} &= -A_1\lambda_1 [\theta - (1 - u_1)\alpha\delta(I + \tau A) [\delta\nu(1 - \alpha)(I + \tau A) + u_4] + \mu] \\ -\frac{\partial H}{\partial E} &= -A_2 + \lambda_2(\beta + u_3) - \lambda_3\beta\lambda - \lambda_4 [\beta(1 - \lambda) + u_3] \\ -\frac{\partial H}{\partial I} &= -A_3 + \lambda_1 [(1 - u_1)\alpha\delta S + \delta\nu(1 - \alpha)S] - \lambda_2\alpha\delta S(1 - u_1) + \lambda(\gamma_i + \varphi_i + u_2) - \lambda_5\delta\nu(1 - \alpha)S \\ &\quad - \lambda_6\varphi_i - \lambda_7(\gamma_i + u_2) \\ -\frac{\partial H}{\partial A} &= \lambda_1 [(1 - u_1)\alpha\delta\tau S + \delta\nu(1 - \alpha)\tau S] - \lambda_2(1 - u_1)1 - \alpha\delta\tau S + \lambda_4\gamma_a - \lambda_5\delta\nu(1 - \alpha)\tau AS - \lambda_7\gamma_a \quad (25) \\ -\frac{\partial H}{\partial Q} &= -A_4 - \lambda_1\rho + \lambda_5(\rho + \varphi_\nu) + \mu + u_3 - \lambda_6(\varphi_\nu + u_3) \\ -\frac{\partial H}{\partial T} &= \lambda(\gamma_t + \kappa + \mu + u_2) - \lambda_7\gamma_t \\ -\frac{\partial H}{\partial R} &= -A_1\phi + \lambda_7\phi.\end{aligned}$$

The adjoint equation can be written as

$$\begin{aligned}\frac{d\lambda_1}{dt} &= -A_1\lambda_1 [\theta - (1 - u_1)\alpha\delta(I + \tau A) [\delta\nu(1 - \alpha)(I + \tau A) + u_4] + \mu] \\ \frac{d\lambda_2}{dt} &= -A_2 + \lambda_2(\beta + u_3) - \lambda_3\beta\lambda - \lambda_4 [\beta(1 - \lambda) + u_3] \\ \frac{d\lambda_3}{dt} &= -A_3 + \lambda_1 [(1 - u_1)\alpha\delta S + \delta\nu(1 - \alpha)S] - \lambda_2\alpha\delta S(1 - u_1) + \lambda(\gamma_i + \varphi_i + u_2) \\ &\quad - \lambda_5\delta\nu(1 - \alpha)S - \lambda_6\varphi_i - \lambda_7(\gamma_i + u_2)\end{aligned}$$

$$\frac{d\lambda_4}{dt} = \lambda_1 [(1 - u_1)\alpha\delta\tau S + \delta\nu(1 - \alpha)\tau S] - \lambda_2(1 - u_1)1 - \alpha\delta\tau S + \lambda_4\gamma_a - \lambda_5\delta\nu(1 - \alpha)\tau AS - \lambda_7\gamma_a \quad (26)$$

$$\frac{d\lambda_5}{dt} = -A_4 - \lambda_1\rho + \lambda_5(\rho + \varphi_\nu) + \mu + u_3 - \lambda_6(\varphi_\nu + u_3)$$

$$\frac{d\lambda_6}{dt} = \lambda(\gamma_t + \kappa + \mu + u_2) - \lambda_7\gamma_t$$

$$\frac{d\lambda_7}{dt} = -A_1\phi + \lambda_7\phi.$$

□

We next obtain the transversality condition by differentiating H partially with respect to  $u_1, u_2, u_3$  and  $u_4$ .

$$\frac{\partial H}{\partial u_1} = B_1u_1 + \alpha\delta(I + \tau A)S\lambda_1 - \lambda_2\alpha\delta(I + \tau A)S$$

$$\frac{\partial H}{\partial u_2} = B_2u_2 - \lambda_3I - \lambda_6T + \lambda_7I$$

$$\frac{\partial H}{\partial u_3} = B_3u_3 - \lambda_2E + \lambda_4E - \lambda_5Q + \lambda_6Q \quad (27)$$

$$\frac{\partial H}{\partial u_4} = B_4u_4 - \lambda_1S + \lambda_5S$$

On solving equation(27) by setting  $\frac{\partial H}{\partial u_i} = 0$ , where  $i = 1, 2, 3, 4$  and  $u_1 = u_1^*, u_2 = u_2^*, u_3 = u_3^*, u_4 = u_4^*$ , we arrive

$$u_1^* = \frac{(\lambda_2 - \lambda_1)\alpha\delta(I + \tau A)S}{B_1}$$

$$u_2^* = \frac{(\lambda_3 - \lambda_7)I + \lambda_6T}{B_2}$$

$$u_3^* = \frac{(\lambda_2 - \lambda_4)E + (\lambda_5 - \lambda_6)Q}{B_3} \quad (28)$$

$$u_4^* = \frac{(\lambda_{21} - \lambda_5)S}{B_4}$$

Imposing the bounds  $0 \leq u_1 \leq u_{1max}, 0 \leq u_2 \leq u_{2max}, 0 \leq u_3 \leq u_{3max}, 0 \leq u_4 \leq u_{4max}$  with the control, then the optimal control are characterized as

$$\begin{aligned} u_1^*(t) &= \min \{ \max(0, G_1), 1 \} \\ u_2^*(t) &= \min \{ \max(0, G_2), 1 \} \\ u_3^*(t) &= \min \{ \max(0, G_3), 1 \} \\ u_4^*(t) &= \min \{ \max(0, G_4), 1 \} \end{aligned} \quad (29)$$

Thus the control arguments are given in a simpler piecewise for below

$$u_1^* = \begin{cases} G_1, & \text{if } 0 \leq G_1 \leq 1 \\ 0, & \text{if } G_1 < 0, \\ 1, & \text{if } G_1 > 1 \end{cases} \quad (30)$$

$$u_2^* = \begin{cases} G_1, & \text{if } 0 \leq G_2 \leq 1 \\ 0, & \text{if } G_2 < 0, \\ 1, & \text{if } G_2 > 1 \end{cases} \quad (31)$$

$$u_3^* = \begin{cases} G_1, & \text{if } 0 \leq G_3 \leq 1 \\ 0, & \text{if } G_3 < 0, \\ 1, & \text{if } G_3 > 1 \end{cases} \quad (32)$$

$$u_4^* = \begin{cases} G_1, & \text{if } 0 \leq G_4 \leq 1 \\ 0, & \text{if } G_4 < 0, \\ 1, & \text{if } G_4 > 1 \end{cases} \quad (33)$$

where

$$G_1 = \frac{(\lambda_2 - \lambda_1)\alpha\delta(I + \tau A)S}{B_1}$$

$$G_2 = \frac{(\lambda_3 - \lambda_7)I + \lambda_6 T}{B_2}$$

$$G_3 = \frac{(\lambda_2 - \lambda_4)E + (\lambda_5 - \lambda_6)Q}{B_3}$$

$$G_4 = \frac{(\lambda_{21} - \lambda_5)S}{B_4}$$

The optimality system derived from the optimal control system (the state variable and the adjoint variables) incorporated with the characterized controls, together with the initial and transversality conditions are used in the numerical simulations.

## 8. Numerical simulations and discussion of results

To tackle this optimal control problem numerically, we leverage a powerful combination of techniques. The iterative sweep method refines solutions through a series of calculations, while the fourth-order forward-backward Runge-Kutta scheme (RK4), adept at handling differential equations with both starting and ending conditions, provides highly accurate solutions at each step. A combination of these approaches ensures that we find the optimal control strategy for the COVID-19 model.

Intuitively, the iterative sweep method provides a systematic way to solve the complex system of equations generated by PMP. On the other hand, the RK4 method ensures accurate numerical solutions for the state and co-state variables. Overall, these approaches help determine the optimal control strategies for mitigating COVID-19 spread by minimizing the chosen cost function within the defined model framework.

To illustrate the impact of different optimal control intervention strategies on a given population, the following control measures are considered to curtail the transmission of COVID-19.

- (i) Strategy 1: Using  $u_1 = 0, u_2 = 0, u_3 = 0, u_4 = 0$
- (ii) Strategy 2: Using  $u_1 = 0, u_2 = 0, u_3 = 0, u_4 \neq 0$
- (iii) Strategy 3: Using  $u_1 = 0, u_2 = 0, u_3 \neq 0, u_4 = 0$

- (iv) Strategy 4: Using  $u_1 = 0, u_2 \neq 0, u_3 = 0, u_4 = 0$
- (v) Strategy 5: Using  $u_1 \neq 0, u_2 = 0, u_3 = 0, u_4 = 0$
- (vi) Strategy 6: Using  $u_1 \neq 0, u_2 \neq 0, u_3 = 0, u_4 = 0$
- (vii) Strategy 7: Using  $u_1 \neq 0, u_2 = 0, u_3 \neq 0, u_4 = 0$
- (viii) Strategy 8: Using  $u_1 \neq 0, u_2 = 0, u_3 = 0, u_4 \neq 0$
- (ix) Strategy 9 : Using  $u_1 = 0, u_2 \neq 0, u_3 \neq 0, u_4 = 0$
- (x) Strategy 10: Using  $u_1 = 0, u_2 \neq 0, u_3 = 0, u_4 \neq 0$
- (xi) Strategy 11: Using  $u_1 \neq 0, u_2 = 0, u_3 = 0, u_4 \neq 0$
- (xii) Strategy 12: Using  $u_1 = 0, u_2 \neq 0, u_3 = 0, u_4 \neq 0$
- (xiii) Strategy 13: Using  $u_1 = 0, u_2 = 0, u_3 \neq 0, u_4 \neq 0$
- (xiv) Strategy 14: Using  $u_1 \neq 0, u_2 = 0, u_3 \neq 0, u_4 \neq 0$
- (xv) Strategy 15: Using  $u_1 = 0, u_2 \neq 0, u_3 \neq 0, u_4 \neq 0$
- (xiv) Strategy 16: Using  $u_1 \neq 0, u_2 \neq 0, u_3 \neq 0, u_4 \neq 0$

The parameter values from Table 1 are used such that  $R_0 = 12.0565$  with initial conditions  $S(0) = 5386$ ,  $E(0) = 995$ ,  $A = 0$ ,  $I(0) = 0$ ,  $Q(0) = 0$ ,  $T(0) = 0$  and  $R(0) = 30$ . The weight constants values are carefully chosen such that  $B_1 = 40$ ,  $B_2 = 50$ ,  $B_3 = 30$ ,  $W_1 = 50$ ,  $W_2 = 50$ ,  $W_3 = 50$ . Just like how we set starting conditions based on what we see in nature, finding the ideal weights for this problem might involve some back-and-forth adjustments. There is no one-size fits-all answer. The key is to select weights that give a solution that best balances the important factors and goals of this particular optimal control problem.

To demonstrate the influence of various optimal control interventions on disease spread, we analyze the impact of 16 different COVID-19 control measures on both asymptomatic and symptomatic infected individuals.

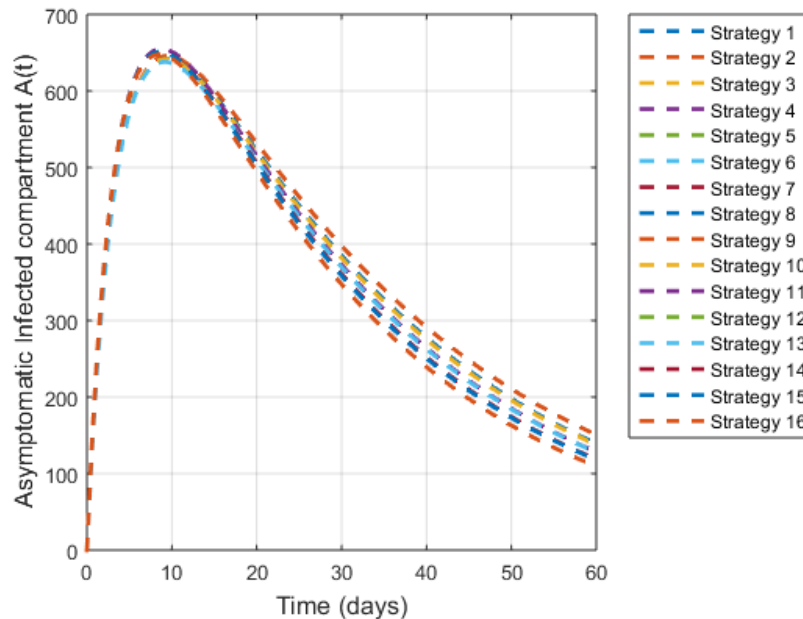


Figure 2. Plot of asymptomatic infected compartment with application of control strategies.

The plot of asymptomatic infected compartment against time is displayed in Figure 2. The graph reveals the effect of all the 16 adopted strategies on the infected compartment, all the strategies have same effect till day 8, which there arises a bit significant difference among some of the controlled strategies. The peak of the infection is at day 10, after which the curve slopes downwards gradually, signifying the effect of the control strategies applied. Strategy 10, strategy 13 and strategy 16 have reduced number of infected individual, thus recommended for the



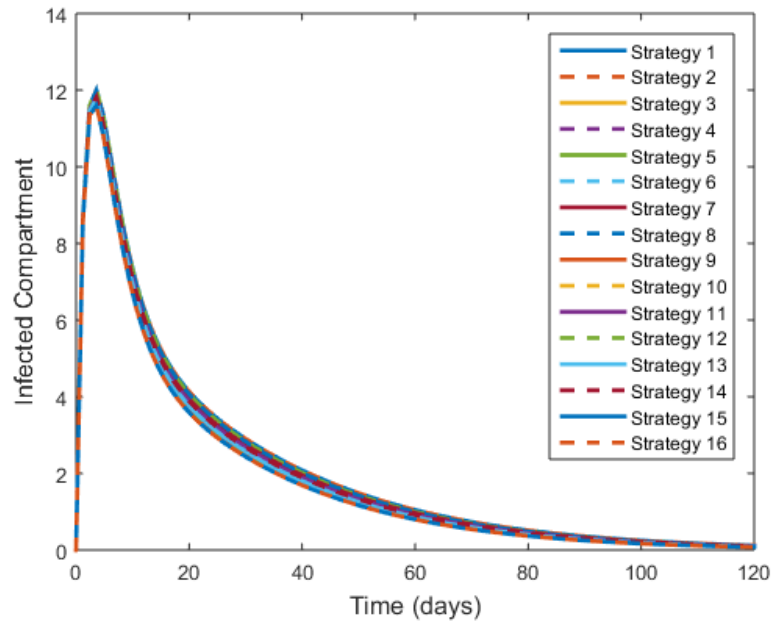


Figure 3. Plot of symptomatic infected compartment with application of control strategies.

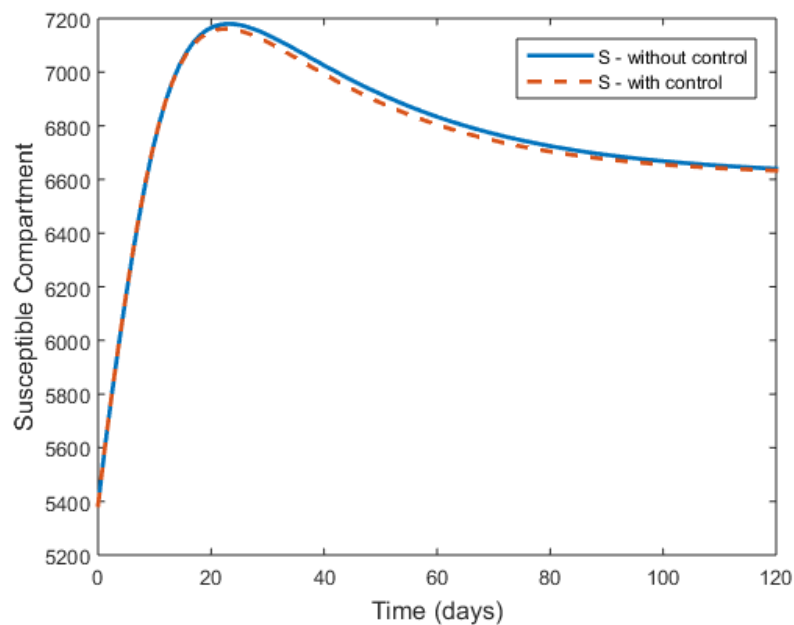


Figure 4. Plot of susceptible individuals against time with control.

treatment of the infected class. Figure 3 displays the plot of symptomatic infected compartment against time, the graph reveals the effect of all the 16 adopted strategies on the infected, strategy 9, strategy 12, strategy 15 and strategy 16 have reduced number of infected individual, thus recommended for the treatment of this infected class.

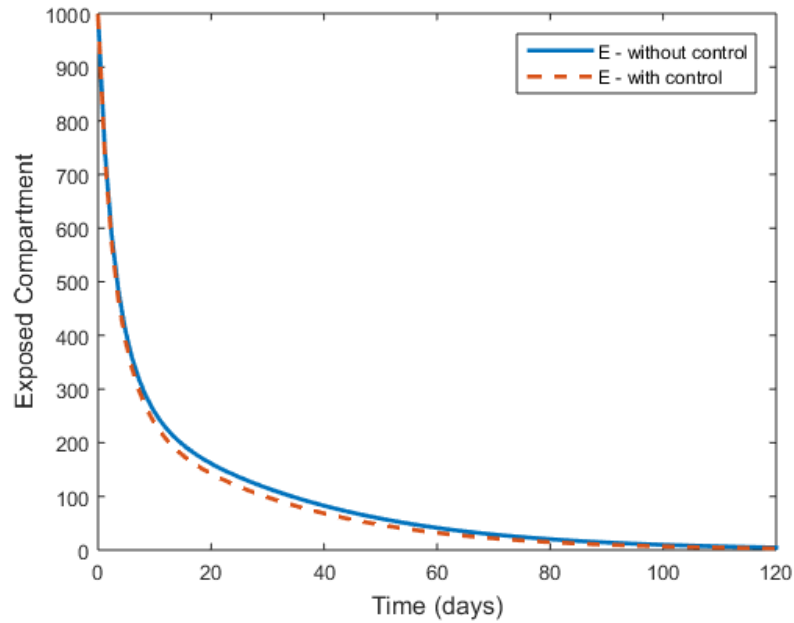


Figure 5. Plot of exposed individuals against time with control.

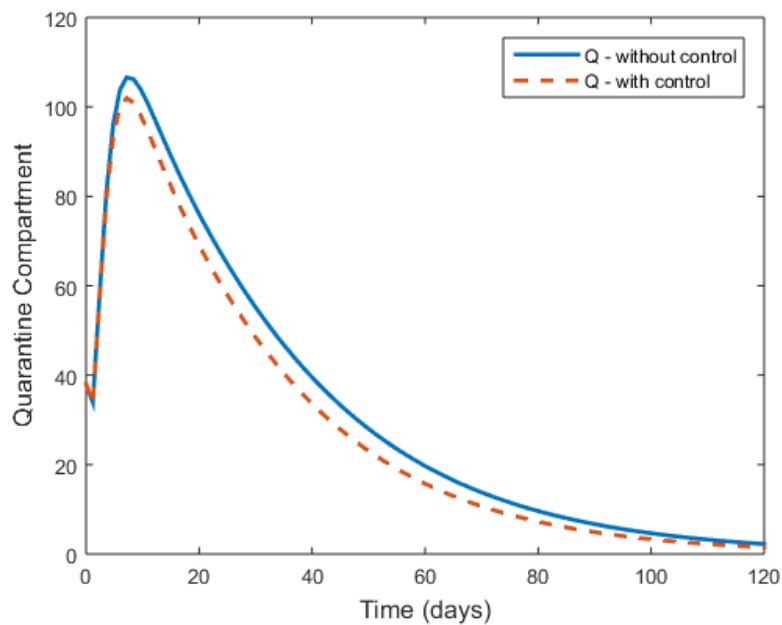


Figure 6. Plot of quarantined uninfected individuals against time.

Considering the scenarios of with and without control measures, Figures 4 and 5 illustrate the changes in the susceptible population over time and exposed population over time, respectively. Initially, in Figure 4, for the first 20 days, both curves show an increase in susceptible individuals, with no significant difference between the two groups. However, after day 20, the curves diverge. The scenario with control measures shows a steeper decline,

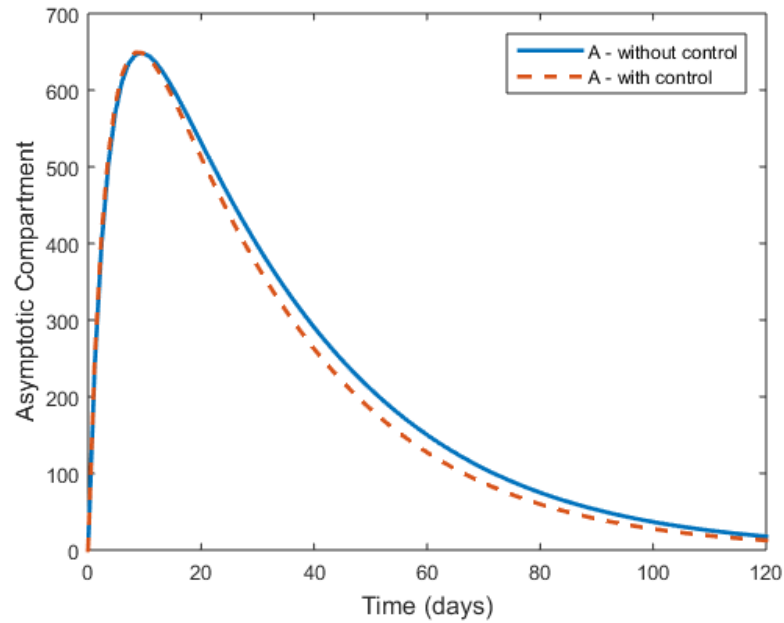


Figure 7. Plot of asymptomatic infected individuals against time.

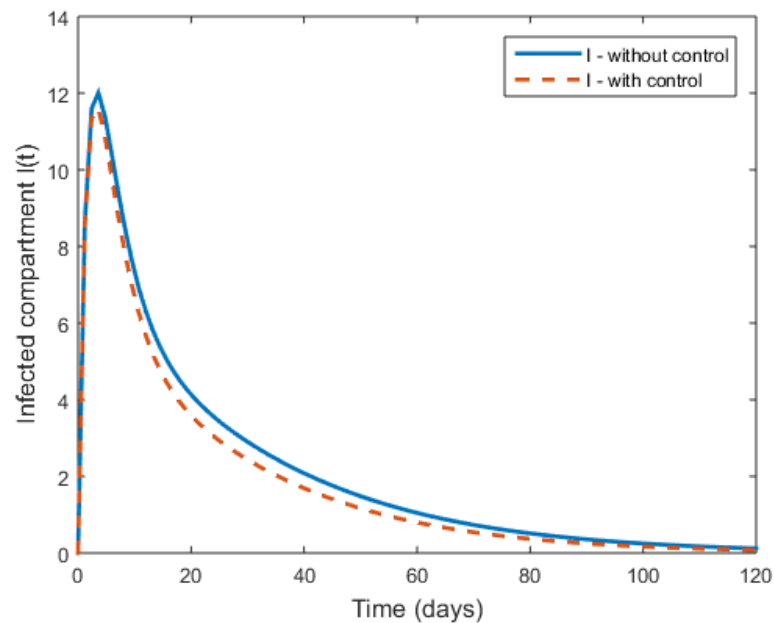


Figure 8. Plot of symptomatic infected individuals against time.

indicating the effectiveness of interventions in reducing the number of susceptible individuals. With respect to Figure 5, both curves initially show a gradual decline without any significant difference until day 17. However, after day 17, a slight divergence emerges, with the control measures scenario exhibiting a steeper decrease in

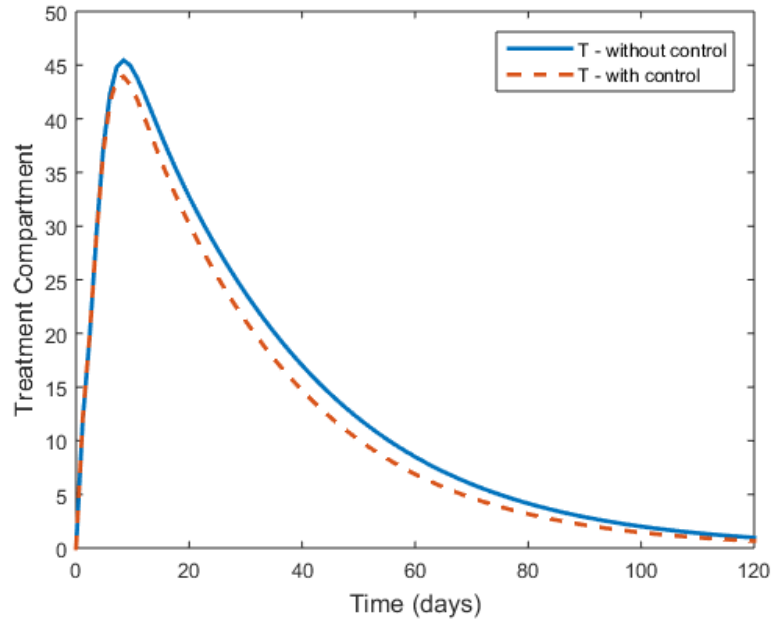


Figure 9. Plot of treated individuals against time.

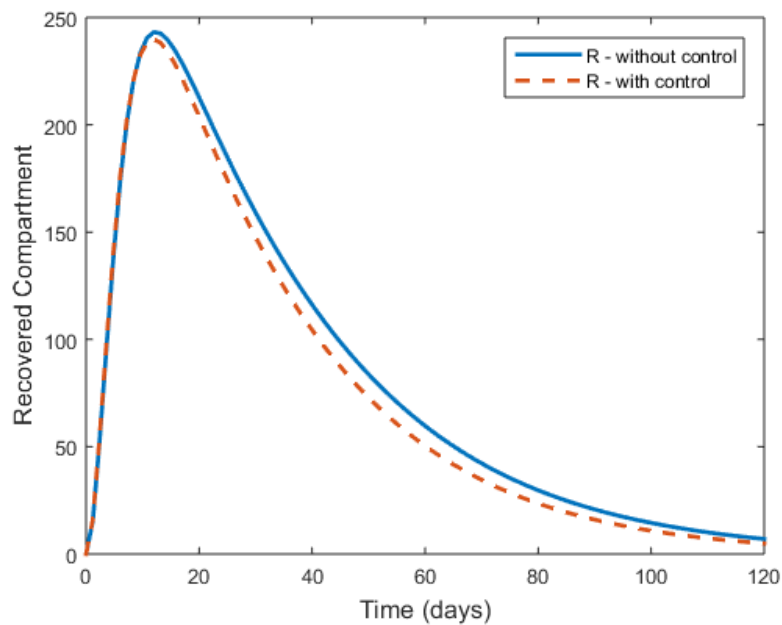


Figure 10. Plot of recovered individuals against time.

exposed individuals. This trend continues until day 104, at which point the number of exposed individuals in both scenarios becomes statistically indistinguishable.

On its own part, Figure 6 illustrates the change in asymptomatic infections over time, modeled with and without control measures. Both curves initially rise, reaching a peak around day 18. There is no major difference between

the curves up to this point, suggesting that control measures have a limited effect on asymptomatic cases during the early stages. However, after day 18, the curves begin to diverge. The scenario with control measures shows a slightly steeper decline, indicating that interventions may lead to a modest reduction in the number of asymptomatic individuals over time. Figure 7 shows the trend in quarantined uninfected contacts over time, considering both scenarios with and without control measures. The curves for both scenarios rise initially, reaching a peak around day 18. Notably, there is no substantial difference between the two curves up to this point. However, after day 18, the curves diverge. The scenario with control measures shows a more pronounced decline, indicating the effectiveness of interventions in reducing the number of quarantined uninfected contacts.

Figure 8 depicts the trajectory of symptomatic infections over time, modeled with and without control measures. Interestingly, both curves rise initially and peak around day 6, suggesting that control measures have minimal impact during this early phase. However, after day 6, the curves diverge significantly. The scenario with control measures shows a steeper decline in infections, indicating the effectiveness of interventions in reducing the number of symptomatic individuals. Figure 9 shows the change over time in the number of treated individuals, with and without control measures implemented. The treated population steadily increases until day 18, followed by a gradual decline. Finally, Figure 10 illustrates the trajectory of recovered individuals over time. The plot shows a rise in the number of recovered individuals until day 18, followed by a gradual decline. This pattern highlights the impact of control measures.

## 9. Conclusion

Mathematical models coupled with optimal control theory provide a powerful framework for analysing COVID-19 transmission dynamics and designing effective control strategies. This article explored a model that incorporates key factors like susceptible population reduction through vaccination and early intervention with medications. By analysing the model, we gained insights into the interplay between these interventions and their impact on disease spread. The application of optimal control techniques allowed us to identify strategies that minimise infection rates while considering practical constraints. The findings from this study can inform public health decision-making. The model can be further refined as our understanding of COVID-19 evolves, allowing for continuous optimisation of control measures. Future directions include incorporating additional factors such as viral mutations and the emergence of new variants. In conclusion, this mathematical modelling approach offers a valuable tool for guiding public health efforts in mitigating the spread of COVID-19 and similar infectious diseases.

## REFERENCES

1. M. Abdullah Bin Masud, A. Mostak, and M. Habibur Rahman, *Optimal control for a COVID-19 model with long quarantine and travel restrictions*, Mathematical Modelling of Natural Phenomena, vol. 15, no. 1, pp. 1–22, 2020.
2. O. J. Adeleke, A. E. Ezugwu, and I. A. Osinuga, *A New Family of Hybrid Conjugate Gradient Methods for Unconstrained Optimization*, Statistics, Optimization and Information Computing, Vol.9, pp. 399–417, 2021.
3. O. J. Adeleke, and M. M. Ali, *An Efficient Model for Locating Solid Waste Collection Sites in Urban Residential Areas*, International Journal of Production Research, vol. 59, no. 3, pp. 798–812, 2021.
4. H. Adedeji-Adenola, O. A. Olugbake, and S. A. Adeosun, *Factors influencing COVID-19 vaccine uptake among adults in Nigeria*, PLoS ONE, vol. 17, no. 1, 26–43, 2022.
5. A. O. Adeniran, A. S. Onanaye, and O. J. Adeleke, *Optimal control of Cocoa Blackpod disease: A multi-pronged approach*, Franklin Open, vol. 7, 100100, 2024.
6. A. O. Adeniran, A. S. Onanaye, O. J. Adeleke and M. Odekunle, *Sensitivity Analysis and Optimal Control of Cocoa Black Pod Disease Caused by Phytophthora Margakarya*, Contemporary Mathematics, vol. 5, no. 2, pp. 2255–2280, 2024.
7. A. O. Adeniran, A. S. Onanaye, and O. J. Adeleke, *Mathematical Model for Spread and Control of Cocoa Black Pod Disease*, Contemporary Mathematics, vol. 4, no. 3, pp. 549–68, 2023.
8. M. E. Adeosun, B. Awoniran, J. A. Akingbade, *A novel mathematical model curbing the spread of COVID-19 in Nigeria*, International Journal of Mathematics Trends and Technology, vol. 68, no. 12, pp. 74–99, 2022.
9. M. C. Agarana, E. A. Owoloko, and O. J. Adeleke, *Optimizing Public Transport Systems in Sub-saharan Africa Using Operational Research Technique: A Focus on Nigeria*, Procedia Manufacturing, vol. 7, pp. 590–595, 2017.
10. J. A. Akingbade, and B. S. Ogundare, *Boundedness and stability properties of solutions of mathematical model of measles*, Tamkang Journal of Mathematics, vol. 51, no. 1, pp. 91–112, 2021.

11. J. Amzat, K. Aminu, V. I. Kolo, A. A. Akinyele, J. A. Ogundairo, and M. C. Danjibo, *Coronavirus outbreak in Nigeria: Burden and socio-medical response during the first 100 days*, International Journal of Infectious Diseases, vol. 98, pp. 218–224, 2020.
12. B. Seidu, *Optimal strategies for control of COVID-19: A mathematical perspective*, Hindawi, vol. 2020.
13. F. Brauer, *Mathematical epidemiology: past, present, and future*, Infectious disease modelling, vol. 2, pp. 113–127, 2017.
14. N. Chitnis, J. M. Hyman, and J. M. Cushing, *Determining important parameters in the spread of malaria through the sensitivity analysis of a mathematical model*, Bulletin of Mathematical Biology, vol. 70, pp. 1272–1296, 2008.
15. A. E. Ezugwu, O. J. Adeleke, and S. Viriri, *Symbiotic Organisms Search Algorithm for Parallel Machine Scheduling*, Plos One, vol. 13, no. 7, 2018.
16. A. E. Ezugwu, O. J. Adeleke, A. A. Akinyelu, and S. Viriri, *Conceptual and numerical comparison of several metaheuristic algorithms on continuous optimization problems*, Neural Computing and Application, pp. 1–45, 2019.
17. E. Goldstein, M. Lipsitch, and M. Cevik, *On the effect of age on the transmission of SARS-CoV-2 in households, schools, and the community*, Journal of Infectious Diseases, vol. 223, no. 3, pp. 362–369, 2021.
18. H. E. Gervas, N. K. Opoku, and S. Ibrahim, *Mathematical modelling of human African trypanosomiasis using control measures*, Computational and Mathematical Methods in Medicine, pp. 1–13, 2018, 5293568.
19. M. Hamidouche, *Mathematical modeling of the COVID-19 outbreak in Algeria*, Chaos, Solitons & Fractals, vol. 138, 2020, 110073.
20. W. H. Herbert, *The mathematics of infectious diseases*, SIAM Review, vol. 42, no. 4, pp. 599–653, 2000.
21. A. Hugo, O. D. Makinde, S. Kumar, and F. F. Chibwana, *Optimal control and cost effectiveness analysis for Newcastle disease eco-epidemiological model in Tanzania*, Journal of Biological Dynamics, vol. 11, no. 1, pp. 190–209, 2017.
22. S. A. Kemp, D. A. Collier, R. Datir, I. Ferreira, A. Carabelli, W. Harvey, ..., and R. K. Gupta, *SARS-CoV-2 evolution during treatment of chronic infection*, Nature, vol. 592, no. 7853, pp. 277–282, 2021.
23. Q. Li, X. Guan, P. Wu, X. Wang, L. Zhou, ..., and Z. Feng, *Early transmission dynamics in Wuhan, China, of novel coronavirus-infected pneumonia*, Lancet, vol. 395, no. 10231, pp. 1473–1477, 2020.
24. S. Mandal, T. Bhatnagar, N. Arinaminpathy, A. Agarwal, A. Chowdhury, M. Murhekar, ..., and S. Sarkar, *Prudent public health intervention strategies to control the coronavirus disease 2019 transmission in India: A mathematical model-based approach*, Indian Journal of Medical Research, vol. 151, no. 2, pp. 190–199, 2020.
25. C. Modnak, *Mathematical modeling of an avian influenza: optimal control study for intervention strategies*, Applied Mathematics & Information Sciences, vol. 11, no. 4, pp. 1049–1057, 2017.
26. A. J. Mumbu, and A. K. Hugo, *Mathematical Modelling on COVID-19 Transmission with Preventive Measures: A Case Study of Tanzania*, Journal of Biological Dynamics, vol. 14, no. 1, 748–766, 2020.
27. S. I. Oke, M. B. Matadi, and S. S. Xulu, *Optimal control analysis of a mathematical model for breast cancer*, Mathematical and Computational Applications, vol. 23, no. 21, pp. 1–28, 2018.
28. D. A. Oladepo, O. J. Adeleke, and C. T. Ako, *A mixed hybrid conjugate gradient method for unconstrained engineering optimization problems*. In: Silhavy R. (eds) Cybernetics and Algorithms in Intelligent Systems. CSOC2018 2018. Advances in Intelligent Systems and Computing, vol. 765. 2019. Springer, Cham.
29. L. S. Pontryagin, V. G. Boltyanskii, and R. V. Gamkrelidze, E. F. Mishchenko, *The Mathematical Theory of Optimal Processes*, Wiley, New York, 1962.
30. L. S. Pontryagin, V. G. Boltyanskii, R. V. Gamkrelidze, and E. F. Mishchenko, *The mathematical theory of optimal control*, American Mathematical Society; 2018.
31. A. Ramponi, and M. E. Tessitore, *Optimal social and vaccination control in the SVIR epidemic model*, Mathematics, vol. 12, no. 7, pp. 933–953, 2024.
32. C. M. Saad-Roy, C. E. Wagner, R. E. Baker, S. E. Morris, J. Farrar, ..., and C. J. E. Metcalf, *Immune life history, vaccination, and the dynamics of SARS-CoV-2 over the next 5 years*, Science, vol. 370, no. 6518, pp. 811–818, 2021.
33. S. M. Salihu, *Mathematical Modeling of COVID-19 Epidemic with Effect of Awareness Programs*, Infectious Disease Modelling, vol. 6, no. 7, pp. 448–460, 2021.
34. B. Seidu, *Optimal strategies for control of COVID-19: A mathematical perspective*, Scientifica, 2020, 4676274.
35. K. K. To, I. F. Hung, J. D. Ip, A. W. Chu, W. M. Chan, ..., and K. Y. Yuen, *COVID-19 re-infection by a phylogenetically distinct SARS-coronavirus-2 strain confirmed by whole genome sequencing*, Clinical Infectious Diseases, vol. 10, 2020.
36. J. P. Townsend, H. B. Hassler, Z. Wang, S. Miura, J. Singh, S. Kumar, ..., and M. Lipsitch, *The durability of immunity against reinfection by SARS-CoV-2: a comparative evolutionary study*, The Lancet Microbe, vol. 2, no. 12, pp. 666–675, 2021.
37. P. Van Den Driessche, and J. Watmough, *Reproduction numbers and the sub-threshold endemic equilibria for compartmental models of infectious disease transmission*, Mathematical Biosciences, vol. 180, pp. 29–48, 2002.
38. World Health Organization. (2020, January 30). Statement on the second meeting of the International Health Regulations (2005) Emergency Committee regarding the outbreak of novel coronavirus (2019-nCoV). <https://news.un.org/en/story/2023/05/1136367>
39. A. Zeb, E. Alzahrani, V. Erturk, and G. Zaman, *Mathematical model for coronavirus disease 2019(COVID 19) containing isolation class*, BioMed research international, vol. 1, 2020. 3452402.
40. K. Zenebe, O. Shiferaw, and L. L. Obsu, *Mathematical Modeling for COVID-19 Transmission Dynamics: A Case Study in Ethiopia*, Results in Physics, vol. 34, pp. 105–191, 2022.
41. N. Zhu, D. Zhang, W. Wang, X. Li, B. Yang, ..., and W. Tan, *A novel coronavirus from patients with pneumonia in China, 2019*, New England Journal of Medicine, vol. 382, no. 8, pp. 727–733, 2020.